J|A|C|S ARTICLES

Published on Web 12/04/2008

$CaFeO_2$: A New Type of Layered Structure with Iron in a Distorted Square Planar Coordination

Cédric Tassel,[‡] José Miguel Pruneda,[†] Naoaki Hayashi,[§] Takashi Watanabe,[‡] Atsushi Kitada,[‡] Yoshihiro Tsujimoto,[‡] Hiroshi Kageyama,*[,‡] Kazuyoshi Yoshimura,[‡] Mikio Takano,[¶] Masakazu Nishi,[⊥] Kenji Ohoyama,[&] Masaichiro Mizumaki,[#] Naomi Kawamura,[#] Jorge Íñiguez,[†] and Enric Canadell*[,†]

Department of Chemistry, Graduate School of Science, Kyoto University, Kyoto 606-8502, Japan, Institut de Ciència de Materials de Barcelona (CSIC), Campus UAB, 08193 Bellaterra, Spain, Graduate School of Human and Environmental Studies, Kyoto University, Kyoto 606-8501, Japan, Institute for Integrated Cell-Materials Sciences and Research Institute for Production Development, 15 Moritomo, Shimogamo, Sakyo, Kyoto 606-0805, Japan, Institute for Solid State Physics, University of Tokyo, 5-1-5 Kashiwanoha, Kashiwa, Chiba 277-8581, Japan, Institute for Materials Research, Tohoku University, 2-1-1 Katahira, Aoba-ku, Sendai 980-8577, Japan, and Japan Synchrotron Radiation Research Institute, SPring-8, Sayo, Hyogo 679-5198, Japan.

Received September 11, 2008; E-mail: kage@kuchem.kyoto-u.ac.jp; canadell@icmab.es

Abstract: $CaFeO_2$, a material exhibiting an unprecedented layered structure containing $3d^6$ iron in a high-spin distorted square-planar coordination, is reported. The new phase, obtained through a low-temperature reduction procedure using calcium hydride, has been characterized through powder neutron diffraction, synchrotron X-ray diffraction, Mössbauer spectroscopy, XAS experiments as well as first-principles DFT calculations. The XAS spectra near the Fe-K edge for the whole solid solution $(Sr_{1-x}Ca_x)FeO_2$ supports that iron is in a square-planar coordination for $0 \leq x \leq 0.8$ but clearly suggests a change of coordination for $x = 1$. The new structure contains infinite FeO_2 layers in which the FeO_4 units unprecedentedly distort from square-planar toward tetrahedra and rotate along the *c*-axis, in marked contrast to the well-studied and accepted concept that octahedral rotation in perovskite oxides occurs but the octahedral shape is kept almost regular. The new phase exhibits high-spin configuration and *G*-type antiferromagnetic ordering as in $SrFeO_2$. However, the distortion of the FeO_2 layers leads to only a slight decrease of the Néel temperature with respect to $SrFeO_2$. First-principles DFT calculations provide a clear rationalization of the structural and physical observations for $CaFeO_2$ and highlight how the nature of the cation influences the structural details of the $AFeO_2$ family of compounds (A = Ca, Sr, Ba). On the basis of these calculations the driving force for the distortion of the FeO_2 layers in $CaFeO_2$ is discussed.

Introduction

The coordination geometries usually exhibited by iron in oxides are octahedral and tetrahedral.[1] However, the use of calcium hydride as a low-temperature reductant, a technique recently introduced by Hayward, Rosseinsky, and co-workers,[2] has provided a way to circumvent this structural choice. For instance, Tsujimoto et al.[3] have recently reported a new material, $SrFeO_2$, in which a high-spin Fe^{2+} exhibits a square-planar coordination. This material is built from unprecedented FeO_2 infinite layers in between which the Sr^{2+} cations reside (see Figure 1) and exhibits a number of surprising structural and physical properties. The study of the electronic structure of $SrFeO_2$ has provided important clues to understand this situation.[4,5] Later, this material was shown to be remarkably robust

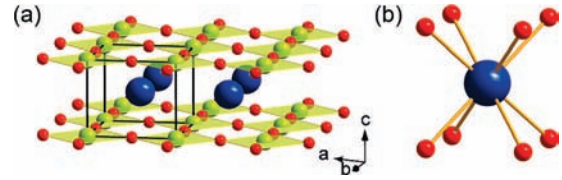

Figure 1. (a) Ideal infinite layer structure $SrFeO_2$. The orange, blue, and green balls are, respectively, oxygen, strontium, and iron atoms. The lines represent the unit cell. (b) Coordination around strontium.

[‡] Graduate School of Science, Kyoto University.
[†] ICMAB (CSIC), Bellaterra.
[§] Graduate School of Human and Environmental Studies, Kyoto University.
[¶] iCeMS.
[⊥] Institute for Solid State Physics, University of Tokyo.
[&] Tohoku University.
[#] SPring-8.

(1) Wells, A. F. *Structural Inorganic Chemistry*, 5th ed.; Oxford University Press: Oxford, U.K., 1984.
(2) (a) Hayward, M. A.; Green, M. A.; Rosseinsky, M. J.; Sloan, J. *J. Am. Chem. Soc.* **1999**, *121*, 8843. (b) Hayward, M. A.; Cussen, E. J.; Claridge, J. B.; Bieringer, M.; Rosseinsky, M. J.; Kiely, C. J.; Blundell, S. J.; Marshall, I. M.; Pratt, F. L. *Science* **2002**, *295*, 1882. (c) Blundred, G. D.; Bridges, A. B.; Rosseinsky, M. J. *Angew. Chem., Int. Ed.* **2004**, *43*, 3562. (d) Bowman, A.; Allix, M.; Pelloquin, D.; Rosseinsky, M. J. *J. Am. Chem. Soc.* **2006**, *128*, 12606.
(3) Tsujimoto, Y.; Tassel, C.; Hayashi, N.; Watanabe, T.; Kageyama, H.; Yoshimura, K.; Takano, M.; Ceretti, M.; Ritter, C.; Paulus, W. *Nature* **2007**, *450*, 1062.
(4) Xiang, H. J.; Wei, S.-H.; Whangbo, M.-H. *Phys. Rev. Lett.* **2008**, *100*, 167207.

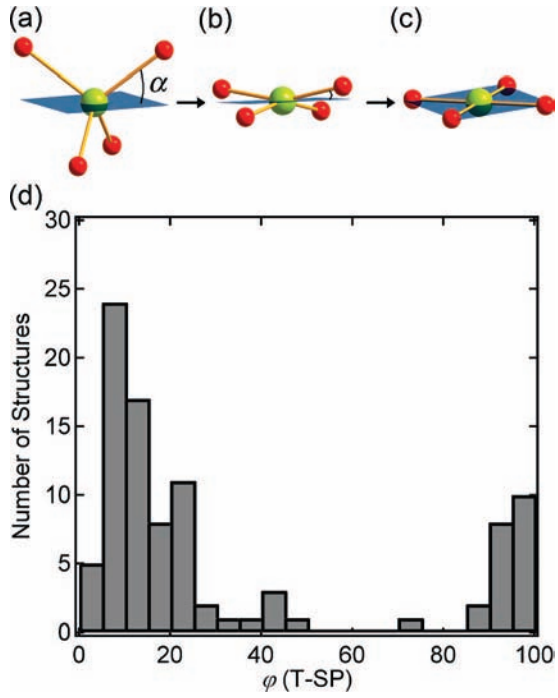

Figure 2. Spread distortion pathway from (a) FeO_4 tetrahedral coordination ($\alpha = 35.26°$) to (c) square-planar coordination ($\alpha = 0°$), realized in $SrFeO_2$, through (b) an intermediate coordination. (d) Distribution of the experimental structures converting from tetrahedron to square in the case of d^6 configurations (adapted with permission from ref 8). For definition of φ(T−SP), please see the text. In the new structure of $CaFeO_2$, α is 8.82° corresponding to φ(T−SP) = 78%.

toward cation substitution and temperature,[6] opening the way to tune parameters for possible applications. More recently, the same technique was used to prepare a new spin-ladder iron oxide, $Sr_3Fe_2O_5$, which again exhibits high-spin Fe^{2+} ions in a square-planar coordination.[7]

In view of the presently available information concerning the correlation between spin-state and stereochemistry in four-coordinate transition metal compounds, the preparation of these new solids with high-spin Fe^{2+} in square-planar coordination is surprising. For instance, in recent studies Cirera et al.[8] have clearly showed by means of DFT calculations that σ-bonded, high-spin four-coordinate d^6 transition metal compounds prefer a tetrahedral coordination (T_d symmetry), whereas the square-planar coordination (D_{4h} symmetry) is preferred for the case of an intermediate-spin configuration. When strong π-bonding ligands are used, the tetrahedral coordination is preferred for both high-spin and intermediate-spin configurations. Several distortion pathways from a tetrahedron to a square can be adopted, that is, sawhorse, plier, spread, umbrella, off-axis, etc.[8] The simplest of these and the one that provides a minimum distortion pathway is the spread-type conversion, as illustrated in structures a−c of Figure 2. Experimentally, however, many compounds exhibit significantly distorted tetrahedral geometries (i.e., φ(T−SP) values around 0 in Figure 2d), while only a few distorted square-planar compounds exist (i.e., φ(T−SP) values around 100 in Figure 2d). In addition, the latter occur for intermediate-spin d^6 transition metals but not in the case of a high-spin configuration.[8] Thus, it is very challenging to pursue the development of these unexpected new extended systems using the hydride reduction route.

Very recently some of us reported the results of the substitution study of $(Sr_{1-x}Ca_x)FeO_2$.[6] Powder XRD patterns for the materials with $0 \le x \le 1$ were shown to be very similar to each other. However, some anomalies were observed for $x = 1$. For instance, a deviation of the Vegard's law was noticed for the *c*-axis, and the Rietveld refinement did not provide a sufficiently good fit to the data ($R_{wp} = 6.20\%$ and $\chi^2 = 18.38$). Although initially these observations were attributed to the existence of some structural defects, later it was felt necessary to reexamine the synchrotron X-ray diffraction data and to perform neutron diffraction that allows precise determination of oxygen positions. This led to the discovery of a new type of layered structure. In this contribution we report the structural and physical characterization of this phase (X-ray, neutron diffraction, Mössbauer spectra, and XAS data) as well as a first-principles theoretical study of $CaFeO_2$ which provides a rationalization of the similarities and differences with $SrFeO_2$.

Experimental Section

Synthesis. A precursor $CaFeO_{2.5}$ crystallizing in the Brownmillerite structure was synthesized by a conventional high-temperature ceramic method from predried $CaCO_3$, (99.999%) and Fe_2O_3 (99.99%) purchased from Rare Metallics Co., Ltd. Reactants were mixed in a stoichiometric ratio, pelletized, and fired at 1200 °C for 24 h. Subsequently, the pellets were ground, re-pelletized, and heated for 48 h with one intermediate grinding. The resulting product was pure according to laboratory X-ray diffraction (Mac Science M18XHF). The synthesis of $CaFeO_2$ was performed by reacting $CaFeO_{2.5}$ with CaH_2. $CaFeO_{2.5}$ and CaH_2 were mixed in a 1:2 molar ratio, ground, and pelletized inside an argon-filled glovebox (MBRAUN). The pellet was inserted into a Pyrex tube and evacuated under a residual 1.3×10^{-8} MPa pressure. The sealed tube was inserted in a furnace for 7 days at 280 °C. The product was then washed for 24 h in a solution of methanol and NH_4Cl with a concentration of 0.15 mol/L in order to remove the byproduct CaO and unreacted CaH_2. $SrFeO_2$ and solid solution $(Sr_{1-x}Ca_x)FeO_2$ ($x = 0.2, 0.4, 0.6, 0.8$) for XAS (X-ray absorption spectroscopy) experiments were also prepared in a similar method.

Powder Neutron Diffraction. We performed neutron powder diffraction experiments at room temperature on the Kinken powder diffractometer for high efficiency and high resolution measurements with multicounters, HERMES, of the Institute for Materials Research (IMR), Tohoku University, installed at the guide hall of the JRR-3 reactor in the Japan Atomic Energy Agency (JAEA), Tokai.[9] The incident neutron with a wavelength of 1.82646 Å was monochromatized by the 331 reflection of a vent Ge crystal. The 12′-blank-sample-18′ collimation was employed. A polycrystalline sample of 5 g mass was placed into a vanadium cylinder. Data were collected with step-scan procedure using 150 neutron detectors in a 2θ range from 3° to 153° with a step width of 0.1°.

Synchrotron Powder X-ray Diffraction. The synchrotron powder diffraction experiments were performed at 293 K on the large Debye−Scherrer camera installed at the Japan Synchrotron Radiation Research Institute SPring-8 BL02B2 by using an imaging plate as a detector. Incident beams from a bending magnet were monochromatized to 0.77709 Å. The sample powder with homo-

(6) Tassel, C.; Watanabe, T.; Tsujimoto, Y.; Hayashi, N.; Kitada, A.; Sumida, Y.; Yamamoto, T.; Kageyama, H.; Takano, M.; Yoshimura, K. *J. Am. Chem. Soc.* **2008**, *130*, 3764.
(7) Kageyama, H.; Watanabe, T.; Tsujimoto, Y.; Kitada, A.; Sumida, K.; Kanamori, K.; Yoshimura, K.; Hayashi, N.; Muranaka, M.; Takano, M.; Ceretti, M.; Paulus, W.; Rittewr, C.; André, G. *Angew. Chem., Int. Ed.* **2008**, *47*, 5740.
(8) (a) Cirera, J.; Ruiz, E.; Alvarez, S. *Chem.-Eur. J.* **2006**, *12*, 3162. (b) Cirera, J.; Ruiz, E.; Alvarez, S. *Inorg. Chem.* **2008**, *47*, 2871. (c) Cirera, J.; Alemany, P.; Alvarez, S. *Chem.-Eur. J.* **2004**, *10*, 190.
(9) Ohoyama, K.; Kanouchi, T.; Nemoto, K.; Ohashi, M.; Kajitani, T.; Yamauchi, Y. *Jpn. J. Appl. Phys.* **1998**, *37*, 3319.

geneous granularity prepared by precipitation method was sealed in a Pyrex capillary of 0.2 mm inner diameter. The synchrotron XRD data were collected in a 2θ range from 0° to 75° with a step interval of 0.01°.

Structural Refinement. The crystal and magnetic structure and cell parameters were refined using both synchrotron X-ray and neutron diffraction data at room temperature. The Rietveld method, implemented in the computer program RIETAN-2000, was used.[10] The peak shape model used was a modified split-pseudo-Voigt function. The agreement indices are R-weighted pattern, $R_{wp} = [\sum w_i(y_{io} - y_{ic})^2/\sum w_i(y_{io})^2]^{1/2}$, R-pattern, $R_p = \sum|y_{io} - y_{ic}|/\sum(y_{io})$, R-Bragg factor, $R_I = \sum|I_o(h_k) - I(h_k)|/\sum I_o(h_k)$ and goodness of fit (GOF), $\chi^2 = [R_{wp}/R_{exp}]^2$, where $R_{exp} = [(N - P)/\sum w_i y_{io}^2]^{1/2}$, y_{io} and y_{ic} are the observed and calculated intensities, w_i is the weighting factor, $I_o(h_k)$ and $I(h_k)$ are the observed and calculated integrated intensities, N is the total number of y_{io} data when the background is refined, and P is the number of adjusted parameters. The bond valence sum (BVS) method was applied to estimate the valence of cations using tabulated parameters, $r_0(Fe) = 1.734$ Å and $r_0(Ca) = 1.967$ Å.[11]

Mössbauer Spectroscopy. Mössbauer spectra of $(Sr_{1-x}Ca_x)FeO_2$ were taken under a dynamical vacuum, and the data were collected in transmission geometry by using ^{57}Co/Rh γ-ray source at low temperature in combination with a constant-acceleration spectrometer. The source velocity was calibrated by using pure α-Fe as a control material. The low-temperature measurements of $CaFeO_2$ were carried out using a cryostat, while the high-temperature spectra were taken with a small amount of CaH_2 that was mixed with the $CaFeO_2$ powder to minimize reoxidation into the Brownmillerite phase $CaFeO_{2.5}$ upon being heated. The subspectrum of $CaFeO_{2.5}$ observed at high temperature was compared with the literature. The obtained spectra were fitted by a Lorentzian function.

XAS Experiments. The XAS spectra at Fe K-edge were measured for $(Sr_{1-x}Ca_x)FeO_2$ ($x = 0.0$, 0.2, 0.4, 0.6, 0.8, and 1.0) at BL39XU of SPring-8 in Japan. The beamline was composed of a double monochromator equipped with a diamond 111 crystal and an Rh-coated mirror for eliminating the higher harmonics. The XAS spectra were recorded under transmission mode using ionization chamber at $T = 300$ K. The energy resolution was about 0.5 eV around Fe K-edge.

Computational Details. The first-principles calculations were of the spin-polarized type within the generalized gradient approximation (GGA)[12] to density functional theory (DFT)[13] as implemented in the code VASP,[14] and employed the "LDA+U" correction of Dudarev et al.[15] for the Fe-3d electrons. The value $U = 4$ eV was used since we previously found[5] that it is appropriate for materials like $SrFeO_2$ and checked that our qualitative results are already obtained at the GGA level. The PAW method[16] was used to represent the ionic cores, solving explicitly for the following electrons: 3s, 3p, and 4s of Ca; 3p, 3d, and 4s of Fe; and 2s and 2p of O. The electronic wave functions were described with a plane-wave basis truncated at 400 eV. Typically, we worked with the 16-atom cell depicted in Figure 8 which is compatible with the magnetic ground-state of the system as well as with the experimentally observed unit cell, and used a $4 \times 4 \times 4$ grid for Brillouin zone integrations. These calculations were checked to render accurate results. Two different codes, PWscf[17] and ABINIT,[18] were also used for some of the electronic structure analysis and the electric field gradient calculations, respectively. The LDA+U schemes implemented in PWscf[19] and ABINIT[20] differ in some details from that of Dudarev et al.[15] We have checked that the results do not depend significantly on the specific LDA+U approach used.

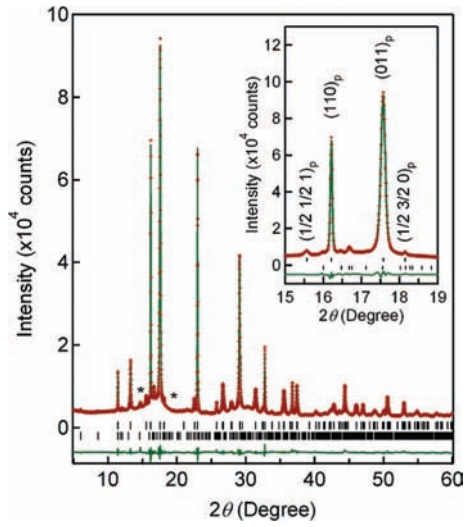

Figure 3. Refined synchrotron powder X-ray diffraction pattern of $CaFeO_2$ showing observed (red crosses), calculated (green line), and difference (bottom) profiles. The black and blue ticks represent the Bragg reflection positions of $CaFeO_2$ and $CaFeO_{2.5}$, respectively. The two stars show unknown impurities. (Inset) Enlarged plot showing the indices with respect to the original $a_p \times a_p \times c_p$ cell.

Results and Discussion

Structure Determination. In the previous report, the synchrotron X-ray diffraction profile of the $CaFeO_2$ sample at room temperature was analyzed assuming the ideal infinite layer structure, using the tetragonal symmetry ($P4/mmm$) with cell parameters being $a_p = 3.89$ Å and $c_p = 3.35$ Å. A small amount of the unreacted $CaFeO_{2.5}$ crystallizing in the Brownmillerite structure and unidentified impurity phases were thought to be present.[6] In this study, it is noticed, however, that some of unidentified weak reflections could be indexed as the super-reflections corresponding to a modulation vector of (1/2, 1/2, 0) with respect to the original tetragonal cell. For example, weak peaks centered at $2\theta = 15.57°$, 18.14°, and 22.58° were assigned as $(1/2\ 1/2\ 1)_p$, $(1/2\ 3/2\ 0)_p$, $(1/2\ 3/2\ 1)_p$, respectively (see the inset of Figure 3). This manifests that the true unit cell of $CaFeO_2$ is written as a tetragonal supercell $\sqrt{2}a_p \times \sqrt{2}a_p \times c_p$. Further analysis of the pattern yielded systematic absences corresponding to an extinction condition $0k0$ (k = odd) based on the new cell. Thus, among tetragonal space groups the possible space groups are $P42_12$ (No. 90) and $P\text{-}42_1m$ (No. 113).

The Rietveld refinement of the synchrotron data was carried out both in the space groups of $P\text{-}42_1m$ and $P42_12$. $CaFeO_{2.5}$

(10) Izumi, F.; Ikeda, T. *Mater. Sci. Forum* **2000**, *321−324*, 198–203.
(11) Brown, I. D.; Altermatt, D. *Acta Crystallogr.* **1985**, *B41*, 244–247.
(12) Perdew, J. P.; Burke, B.; Ernzerhof, M. *Phys. Rev. Lett.* **1996**, *77*, 3865.
(13) (a) Hohenberg, P.; Kohn, W. *Phys. Rev.* **1964**, *136*, B864. (b) Kohn, W.; Sham, L. J. *Phys. Rev.* **1965**, *140*, A1133.
(14) Kresse, G.; Furthmuller, J. *Phys. Rev. B: Condens. Mater. Chem.* **1996**, *54*, 11169.
(15) Dudarev, S. L.; Botton, G. A.; Savrasov, S. Y.; Humphreys, C. J.; Sutton, A. P. *Phys. Rev. B: Condens, Mater. Chem.* **1998**, *57*, 1505.
(16) (a) Blochl, P. E. *Phys. Rev. B: Condens. Mater. Chem.* **1994**, *50*, 17953. (b) Kresse, G.; Joubert, D. *Phys. Rev. B: Condens. Mater. Chem.* **1999**, *59*, 1758.
(17) Baroni, S.; Dal Corso, A.; de Gironcoli, S.; Giannozzi, P., http://www.pwscf.org/.
(18) Gonze, X.; Beuken, J. M.; Caracas, R.; Detraux, F.; Fuchs, M.; Rignanese, G. M.; Sindic, L.; Verstraete, M.; Zerah, G.; Jollet, F.; Torrent, M.; Roy, A.; Mikami, M.; Ghosez, Ph.; Raty, J. Y.; Allan, D. C. *Comput. Mater. Sci.* **2002**, *25*, 478; http://www.abinit.org/.
(19) Cococcioni, M.; de Gironcoli, S. *Phys. Rev. B: Condens. Mater. Chem.* **2005**, *71*, 035105.
(20) Liechtenstein, A. L.; Anisimov, V. I.; Zaanen, J. *Phys. Rev. B: Condens. Mater. Chem.* **1995**, *52*, 5467.

Table 1. Atomic Coordinates and Isotropic Displacement Factors of $CaFeO_2$ from Neutron[a] (upper) and Synchrotron X-ray[b] (lower) Measurements

atom	site	*sof*	*x*	*y*	*z*	$100U_{iso}$
Ca	2*c*	1	0.5	0	0.4373(3)	0.614(1)
					0.4377(2)	0.939(3)
Fe	2*a*	1	0	0	0	0.747(8)
						0.795(2)
O	4*e*	1	0.2275(5)	0.7275(5)	0.0917(5)	1.151(7)
			0.2312(3)	0.7312(3)	0.0943(6)	1.318(6)

[a] $P\text{-}42_1m$, $Z = 2$, $a = 5.5068(1)$ Å, $c = 3.3552(1)$ Å, $R_{wp} = 3.03\%$, $R_p = 2.36\%$, $R_I = 6.27\%$, $\chi^2 = 2.210$. [b] $P\text{-}42_1m$, $Z = 2$, $a = 5.5067(3)$ Å, $c = 3.3564(1)$ Å, $R_{wp} = 2.68\%$, $R_p = 2.05\%$, $R_I = 3.25\%$, $\chi^2 = 3.442$.

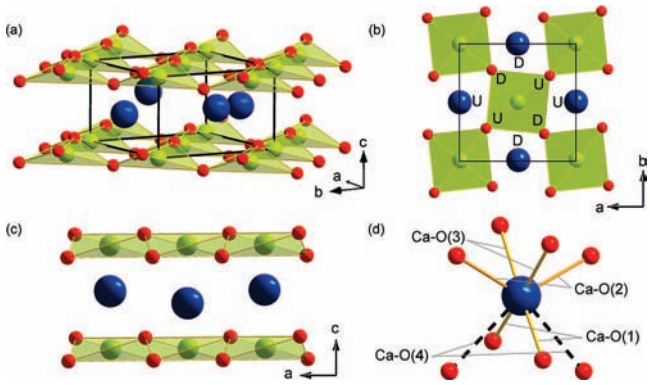

Figure 4. (a) The new structure of $CaFeO_2$. The orange, blue, and green balls are respectively oxygen, calcium, and iron atoms. The solid lines represent the unit cell. (b) [001] and (c) [010] projections. (d) Coordination around calcium atom.

was included in the calculation as the secondary phase using the model described by Berastegui et al.[21] For $P\text{-}42_1m$, we started the refinement with the initial atomic positions, referring to those of the ideal infinite layer structure, i.e., placing Fe on 2*a*, Ca on 2*c* (0, 1/2, *z*) ($z = 0$), and O on 4*e* (*x*, *x*+1/2, *z*) ($x = z = 0$). The refinement immediately converged to $a = 5.5067(3)$ Å, $c = 3.3564(1)$ Å, $z = 0.4377(2)$ for Ca, $x = 0.2312(3)$, $z = 0.0943(6)$ for O, $R_{wp} = 2.68\%$, $R_p = 2.05\%$, $R_I = 3.25\%$, $\chi^2 = 3.442$ along with reasonable individual isotropic displacement factors for all atoms. Setting oxygen occupancies as free parameters revealed that the oxygen site is fully occupied, i.e., *sof* = 1 (*sof* stands for site occupancy factor). Possibilities of disorder for each atom on each site and of partially occupied oxygen atoms in the apical site above the iron were checked, but no improvement of the refinement was obtained. The $CaFeO_{2.5}$ impurity ratio was 4%. The BVS calculation gave +1.88, + 1.95 for Ca and Fe. These values reasonably agree with the expected valences of +2 for those elements and indeed are much improved in comparison with the previous structural model that led to +1.55, + 2.25 for Ca and Fe. All the refined values are listed in Table 1. The observed and calculated patterns and the difference patterns are shown in Figure 3, and Figure 4 illustrates the crystal structure of $CaFeO_2$. The analysis was also conducted for $P42_12$, in a similar way as described above, by placing Fe on 2*a*, Ca on 2*c* (0, 1/2, *z*), and O on 4*e* (*x*, *x*, *z*), which resulted in slightly larger values $R_{wp} = 2.81\%$, $R_p = 2.15\%$, $\chi^2 = 3.792$.

Because the position of the oxygen atoms is the only difference between the two models ($P\text{-}42_1m$ and $P42_12$)

(21) Berastegui, P.; Eriksson, S.-G.; Hull, S. *Mater. Res. Bull.* **2001**, *34*, 303.

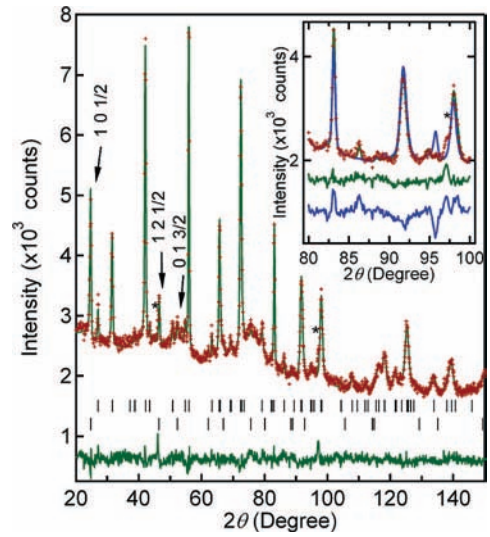

Figure 5. Refined powder neutron diffraction pattern of $CaFeO_2$ showing observed (red crosses), calculated (green line), and difference (bottom) profiles. The upper and lower ticks represent the positions of the calculated chemical and magnetic Bragg reflections. The asterisk shows an unidentified peak. The inset shows the enlarged plot to compare with the calculated and difference profile assuming $P42_12$ (blue).

discussed in the previous paragraphs, the study of the neutron diffraction data is decisive in determining the true structure. In accordance with the synchrotron data, the neutron diffraction patterns at room temperature (Figure 5) were indexed by a tetragonal $\sqrt{2}a_p \times \sqrt{2}a_p \times c_p$ supercell and the extinction condition of $0k0$ (k = odd). Peaks corresponding to $CaFeO_{2.5}$ were not detected within the experimental resolution. Moreover, we observed (π, π, π) magnetic reflections, which were introduced in the following refinement. The details of the magnetic properties will be discussed in the later section. A relatively high background indicates the presence of hydrogen atoms in the sample, which probably is due to an over-reduced noncrystallized phase and/or residual noncrystallized CaO that reacted with water during exposure to air after the hydride reduction. Despite this fact, it is clearly seen that the theoretical profile using $P\text{-}42_1m$ can reproduce the experimental data satisfactorily, providing $R_{wp} = 3.03\%$, $R_p = 2.36\%$, $R_I = 6.27\%$, $\chi^2 = 2.210$ (Figure 5). The refined lattice parameters and atomic coordinates are close to those obtained by the synchrotron X-ray diffraction study. On the other hand, rather poor agreement was obtained for $P42_12$ ($R_{wp} = 5.19\%$, $R_p = 3.97\%$, $R_I = 10.11\%$, $\chi^2 = 6.519$) as seen in the inset of Figure 5. The BVS calculations gave a considerable deviation from the expected valence, +2.25 for Fe and +1.65 for Ca. These observations led us to the conclusion that $P\text{-}42_1m$ is the only possible space group.

Structural Features. It is well-known that perovskite structures ABO_3 are governed by the size of the A site. When the so-called Goldschmidt factor t is close to 1 as in $SrFeO_3$ ($t = 1.02$), one obtains an ideal structure with the cubic $Pm\text{-}3m$ space group, and the A site is 12-fold coordinated by oxygen atoms. When t deviates from 1, tilting or rotating BO_6 octahedra of various types occurs, leading to lowered coordination numbers, lowered symmetries, and superstructures. Here it should be stressed that, upon octahedral rotations, each octahedron tries to keep its rigid shape. In $CaFeO_3$ ($t = 0.956$), for example, uniform rotation along *a*-axis and staggered rotation along *b*- and *c*-axes give an orthorhombic $\sqrt{2}a_p \times \sqrt{2}b_p \times 2c_p$ cell (*Pnma*) to reduce the coordination number of Ca down to 9.

Table 2. Selected Interatomic Distances (Å), Bond Angles (deg) from Neutron (left) and Synchrotron X-ray (right) Measurements

Ca−O(1) × 2	2.374(1)/2.389(1)	Fe−O × 4	1.979(1)/1.978(1)
Ca−O(2) × 2	2.418(1)/2.390(1)	Ca−Fe(1) × 4	3.120(1)/3.121(1)
Ca−O(3) × 2	2.508(1)/2.536(1)	Ca−Fe(2) × 4	3.338(1)/3.338(1)
Ca−O(4) × 2	3.053(1)/3.039(1)	∠Fe−O−Fe	159.39/ 159.69
		∠O−Fe−O	162.11/161.58

Group theory approaches were successfully employed by Glazer, Alexandrov, Woodward and others to predict the relation between octahedral rotations and space groups.[22]

The determined $CaFeO_2$ structure, shown in structures a−c of Figure 4, is characterized not only by the rotation of FeO_4 along the *c*-axis approximately 5 °, but also by the distortion of squares toward tetrahedra. Such a rotation is frequently seen in perovskite oxides, as discussed above, and is responsible for the superlattice formation $\sqrt{2}a_p \times \sqrt{2}a_p \times c_p$. However, in contrast to rigid octahedra in perovskite oxides, each FeO_4 square in the infinite layer structure is remarkably flexible. It is deformed by moving one set of diagonal oxygen atoms up and the other set down along the *c*-axis, relative to the original FeO_2 plane. The ideal infinite layer structure $SrFeO_2$ adopts an eight-fold coordination around Sr (Figure 1b). If the *z* coordinate for calcium in the new structure were 0.5, this deformation would provide 4 short and 4 long Ca−O bonds. In practice, *z* is around 0.43, and as a result, four different pairs of Ca−O bonds are generated (Table 2 and Figure 4d). Since one pair has a distance longer than 3 Å and the other three have distances of around 2.4−2.5 Å, the coordination around Ca is regarded as six-fold. The elongated *c*-axis at $x = 1$ is also explained by considering the movements of Ca and O along the *c*-axis.

A measure of distortion through a spread distortion pathway from a square plane or from a tetrahedron is defined by $\varphi(\mathrm{T-SP}) = 100 \times (1 - \alpha/\theta)$, where α is the angle between an Fe−O bond and a median plane (Figure 2) and $\theta = \arcsin(1/\sqrt{3})$ corresponding to α for a rigid tetrahedron.[8] The value of φ(T−SP) for $CaFeO_2$ is estimated to be 78% ($\alpha = 8.82°$). The distorted square-planar coordination is quite rare since, in general, square-planar coordination is hardly distorted; as illustrated in Figure 2d, only one d^6 complex $[Co(S\text{-}2,4,6\text{-}i\text{-}Pr_3C_6H_2)_4]^-$ in high-spin state is reported to have a similar coordination geometry.[24] This situation is the same for Cu^{II} compounds (d^9). No distortion has been reported in the infinite layer cuprate $ACuO_2$ (A = Ca, Sr, Ba). Completely flat $CuBO_3$ sheets in $SrCu_2(BO_3)_2$ show a corrugation below a structural transition temperature, but each CuO_4 square itself remains almost flat.[23]

The structure of $CaFeO_2$ merits comparison with a recently discovered high-T_c superconducting iron oxypnictide family,[25] where $FeAs_4$ tetrahedra edge-share to form FeAs layers. It is discussed that φ(T−SP) in $FeAs_4$ is distributed in a narrow range of 0−6% ($\alpha = 35.26-33°$), yet T_c is very sensitive to the "tetrahedricity".[26] Although the FeO_4 polyhedron in $CaFeO_2$ with $\varphi(\mathrm{T-SP}) = 78\%$ ($\alpha = 8.82°$) is closer to a square planar than a tetrahedron, it offers an alternative route to form tetrahedral iron layers by corner sharing. Application of strain, for example, may further decrease φ(T−SP) and could induce superconductivity if carriers are allowed to be injected into the layers.

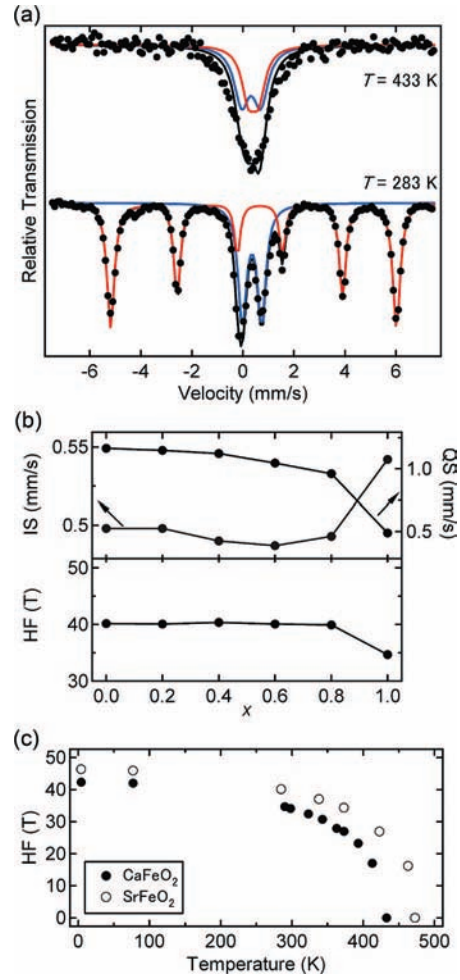

Figure 6. (a) Mössbauer spectra of $CaFeO_2$ at 283 K (lower) and 433 K (upper). The red line indicates the spectra from $CaFeO_2$, the blue line from the amorphous impurity formed during the hydride reduction. The black line is the total fit. (b) The *x* dependence of isomer shift (IS), quadrupole splitting (QS) hyperfine field (HF). (c) The temperature dependence of HF for $CaFeO_2$ (closed) and $SrFeO_2$ (open).

Magnetic Properties. The analysis of the neutron diffraction pattern at room temperature by Rietveld refinement revealed the presence of the (π, π, π) antiferromagnetic (AFM) order (*G*-type), which is the same spin structure as that found in $SrFeO_2$.[3] The magnetic moments are aligned perpendicular to the *c*-axis (within the resolution of the measurements), and have 3.3 μ_B per iron ion, suggesting the high-spin configuration as in the case of $SrFeO_2$.[3] The presence of the magnetic order well above room temperature and the high-spin ($S = 2$) configurations were also evidenced by ^{57}Fe Mössbauer spectrum at 285 K that exhibits six peaks with a hyperfine field of 30 T (Figure 6a). It also supports the magnetic moments lying in the plane.

(22) (a) Glazer, A. M. *Acta Crystallogr., Sect. B* **1972**, *28*, 3384. (b) Aleksandrov, K. S. *Ferroelectrics* **1976**, *14*, 801. (c) Woodward, P. M. *Acta Crystallogr., Sect. B* **1997**, *53*, 32.
(23) Sparta, K.; Redhammer, G. J.; Roussel, P.; Heger, G.; Roth, G.; Lemmens, P.; Ionescu, A.; Grove, M.; Güntherodt, G.; Hüning, F.; Lueken, H.; Kageyama, H.; Onizuka, K.; Ueda, Y. *Eur. Phys. J. B* **2001**, *19*, 507.
(24) Fikar, R.; Koch, S. A.; Millar, M. M. *Inorg. Chem.* **1985**, *24*, 3311.
(25) Kamihara, Y.; Watanabe, T.; Hirano, M.; Hosono, H. *J. Am. Chem. Soc.* **2008**, *130*, 3296.
(26) Lee, C.-H.; Iyo, A.; Eisaki, H.; Kito, H.; Fernandez-Diaz, M. T.; Ito, T.; Kihou, K.; Matsuhata, H.; Braden, M.; Yamada, K. *J. Phys. Soc. Jpn.* **2008**, *77*, 083704.

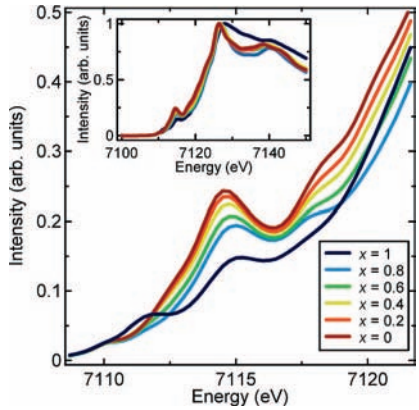

Figure 7. X-ray absorption spectra of the solid solution $Sr_{1-x}Ca_xFeO_2$ ($0 \leq x \leq 1$).

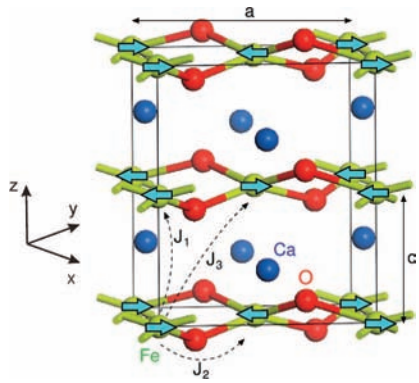

Figure 8. Sixteen-atom unit cell for $CaFeO_2$ used in most of the calculations. The ground-state magnetic structure is presented, and the different exchange couplings are labeled.

Note that a paramagnetic iron-containing phase with a relative area intensity of 40% was observed in the spectrum together with the Brownmillerite phase $CaFeO_{2.5}$. Since both X-ray and neutron diffractograms did not show such an impurity as a crystalline phase, this phase is likely to come from an over-reduced, decomposed amorphous impurity, which is correlated to the enormous difficulty in the synthesis:[6] severe synthetic conditions for reduction—a narrow temperature range (270−300 °C) and a long period of time (>4 days)—are required for the preparation of $CaFeO_2$. This supplies a contrast to the case of $SrFeO_2$ (250−400 °C, less than 1 day), but yet the over-reduced, decomposed amorphous phase was detected also in the Mössbauer spectra of $SrFeO_2$ when the hydride reaction was performed above 350 °C.

Though the difference in magnetism between $SrFeO_2$ and $CaFeO_2$ is less apparent at first glance of neutron diffraction and Mössbauer results, a conspicuous feature of $CaFeO_2$ has been found upon thorough inspection of the solid solution $(Sr_{1-x}Ca_x)FeO_2$. Shown in Figure 6b are isomer shift, quadrupole splitting, and hyperfine field at room temperature plotted as a function of x. All the Mössbauer parameters remain nearly unchanged for $x = 0$, 0.2, 0.4, 0.6, 0.8, but exhibit a jump at $x = 1$, implying that the electronic structure of $CaFeO_2$ is considerably different from that of the rest, in accordance with the deviation from the Vegard's law for the c-axis.[6] The XAS spectra near the Fe-K edge obtained at room temperature are shown in Figure 7 for the whole solid solution $(Sr_{1-x}Ca_x)FeO_2$. From the position of the spectra, which is similar to that found in the epitaxial thin film of $SrFeO_2$ grown by Inoue et al.,[27] we can confirm a divalent state for iron for the solid solution. The structure of the low-energy edge of $(Sr_{1-x}Ca_x)FeO_2$ ($0 \leq x \leq 0.8$) supports that the iron exhibits square-planar coordination. However, the spectrum of $CaFeO_2$ is apparently different, suggesting a brand new coordination and electronic properties.

Table 3. Computed properties of the *P-42₁m* phase of $CaFeO_2$

structure:	$a = b = 5.5155$ Å; $c = 3.3251$ Å		
Fe (2*a*):	0.0	0.0	0.0
Ca (2*z*):	0.5	0.0	0.4206
O (4*e*):	0.2768	0.7768	0.0552
infrared active modes (cm^{-1}):	138, 236, 255, 333, 357 and 549 (*E*) 203, 268 and 495 (B_2)		
magnetic couplings (meV):	$J_1 = 1.30$, $J_2 = 5.24$, $J_3 = -0.06$		

Given the ideal undistorted infinite layer structure of $SrFeO_2$, $CaFeO_2$ has been predicted to display stronger magnetic interactions and higher T_N than $SrFeO_2$.[4] However, the observed smaller value of the isomer shift for $CaFeO_2$ (vs $SrFeO_2$) implies a reduced T_N. To check this, we measured the Mössbauer effects at various temperatures, and found that T_N is around 420 K (Figure 6(c)), which is lower than that of $SrFeO_2$. The discrepancy is naturally understood in terms of the structural modifications, in particular, the bridging angle ∠Fe−O−Fe. Namely, $CaFeO_2$ having ∠Fe−O−Fe = 159.4° would provide a smaller in-plane antiferromagnetic exchange constant J_2 (see Figure 8 for notation) than $SrFeO_2$ having ∠Fe−O−Fe = 180°. This analysis is consistent with our DFT calculations of the magnetic coupling constants reported in the next section.

What is most remarkable is that the reduction in T_N is at most 50 K (10%) in spite of the large deviation of the oxygen bridging angle from 180°. Thus, the (π, π, π) AFM order is robust. In $AMnO_3$ (A = La and rare earth elements), the in-plane bridging angle ∠Mn−O−Mn is tuned by the A site (e.g., 155. 1° for A = La, 148.0° for Sm and 146.2° for Gd), leading to substantially reduced magnetic interactions. As a consequence, the A-type magnetic order temperature is drastically changed (140 K for A = La, 60 K for Nd and 25 K for Gd). This contrasting behavior suggests that hybridization between Fe $d_{x^2-y^2}$ to O p orbitals, which should be mostly relevant to J_2, is not strongly influenced by the bridging angle. Indeed, the isomer shift of $CaFeO_2$ (0.542 mm/s) is very close to that of $SrFeO_2$ (0.498 mm/s) and is much smaller than that reported for iron compounds with divalent iron in high-spin state. This agrees with the results of the first-principles calculations discussed in the next section.

Electronic Structure Calculations and Origin of the Distortion. The observation of the distorted layered structure for $CaFeO_2$ is, at first sight, surprising in view of previous theoretical studies[5] showing that $SrFeO_2$ is stable upon symmetry-lowering structural distortions. We have carried out structural optimizations for $CaFeO_2$ and found that the relaxed structure is indeed nonplanar with a local coordination of the iron atoms in between square-planar and tetrahedral. As experimentally found, the FeO_4 units rotate around the c-axis in a concerted way. The calculated structure (see Table 3) is in excellent agreement with the experimental data. The phonon spectra at the Γ point were calculated, and the results are

(27) Inoue, S.; Kawai, M.; Shimakawa, Y.; Mizumaki, M.; Kawamura, N.; Watanabe, T.; Tsujimoto, Y.; Kageyama, H.; Yoshimura, K. *Appl. Phys. Lett.* **2008**, *92*, 161911.

summarized in Table 3.[28] We did not find modes with imaginary frequencies and can thus conclude that the $P\text{-}42_1m$ phase of $CaFeO_2$ is a stable structure.

We then considered all the spin arrangements compatible with the cell of Figure 8 and found an AFM ground state with the same magnetic order as in $SrFeO_2$ (see Figure 8). The Fe^{2+} ions are in a high-spin configuration with a magnetic moment of 3.6 μ_B, which agrees with the experimental data. The exchange parameters of a model Hamiltonian $H = 1/2\Sigma_{ij}J_{ij}S_iS_j$ with $|S| = 2$ were calculated, and the results are reported in Table 3 (see Figure 8 for notation). In general the coupling constants, J_1, J_2, J_3, in $CaFeO_2$ are slightly weaker than in $SrFeO_2$ although they follow the same trend. As found in that material the intralayer interactions are considerably stronger than those along c; however, even if the material may be considered as two-dimensional from the structural viewpoint, this is not quite true from the magnetic viewpoint. For instance, a rough estimate using a simple mean field approach based on the coupling constants of Table 3 leads to T_N around 1100 K. Although, as expected, T_N is overestimated, this temperature is somewhat smaller than that calculated for $SrFeO_2$ (approximately 1500 K), in agreement with the trend in experimental results. The magnetic coupling between the FeO_2 planes in $CaFeO_2$ is estimated to be around 140 K, which is approximately one-half of that found for $SrFeO_2$.[5] Thus, although the distortion reinforces the structural coupling between layers through stronger oxygen−calcium−oxygen bonding (see the analysis below of the origin of the distortion), the induced rehybridization associated with the loss of the layer planarity leads to some interplane magnetic decoupling. It is worth mentioning that, whereas the calculated J_1, J_2 and J_3 coupling constants (in meV) for $SrFeO_2$ are $J_1 = 1.75$, $J_2 = 6.58$, and $J_3 = -0.26$, those for the undistorted planar $CaFeO_2$ are $J_1 = 2.90$, $J_2 = 7.70$, and $J_3 = -0.40$. Thus, if the planar nature of the FeO_2 layers were kept, one should expect some increase in T_N for $CaFeO_2$. However, as shown in Table 3, the coupling constants for distorted $CaFeO_2$ are smaller than those for both undistorted planar $CaFeO_2$ and $SrFeO_2$, so that a slight decrease is instead expected, in agreement with the experimental results. It is clear that the effect of the reduction of the cation size, which ultimately should lead to an increase of the coupling constants, is overcompensated by the magnetic decoupling resulting from the rehybridization induced by the loss of planarity.

The calculated density of states (DOS) as well as the partial DOS associated with the 3d orbitals of a particular Fe atom for $CaFeO_2$ as well as for $SrFeO_2$ are reported in Figure 9. Although subtle variations in bonding are behind the differences in structural and magnetic behavior, the calculated DOS for the two phases are quite similar both in global shape and in the participation of the different 3d orbitals. The main difference is a larger gap at the Fermi level for $CaFeO_2$, which seems consistent with even stronger Fe−O interactions in the present material. It is obvious from these results that the Fe^{2+} in $CaFeO_2$ is in a high-spin state and the sixth electron resides in the z^2 minority-spin orbital. Thus, the structural distortion has no major effect on the configuration of the Fe^{2+}. We refer the interested reader to our previous analysis[5] of the DOS for $SrFeO_2$ and the subsequent rationalization of the double occupancy of the z^2 orbital for a qualitative understanding of the essential features

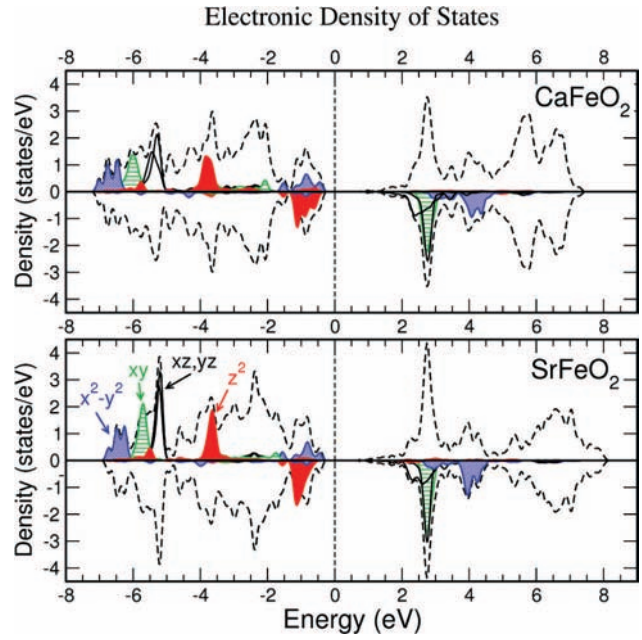

Figure 9. Density of states (DOS) around the Fermi level, which is set to 0 eV, calculated for $CaFeO_2$ and $SrFeO_2$. The partial density of states (pDOS) associated with the different 3d orbitals of a particular Fe atom are also indicated. The black contribution is the total DOS divided by a factor of 4.

of Figure 9. Since the z^2 orbital is nondegenerate, its occupancy in the hypothetical undistorted $CaFeO_2$ planar structure cannot lead to any symmetry-lowering distortion that reduces the energy. The distortion in $CaFeO_2$ must originate from the attempt of the oxygen atoms to optimize the interaction with the interlayer calcium ions.

We also calculated the electric field gradient at the iron site and derived the associated quadrupole splitting which is around 0.20 mm/s. This value is lower than that calculated for $SrFeO_2$, ~0.7 mm/s.[5] These results are in good qualitative agreement with the experimental results and thus clearly show that, even if relatively small, the rearrangement of the electronic structure associated with the distortion is well captured by the present calculations. In addition these results definitely show that the small values of the quadrupole splitting experimentally found for systems like $CaFeO_2$ and $SrFeO_2$ are compatible, even if surprisingly so, with high-spin Fe^{2+} and double occupation of the z^2 orbital.

In order to better understand the origin of the distortion we then carried out calculations for $CaFeO_2$, assuming an idealized planar structure ($a = 5.5699$ Å, $c = 3.1894$ Å). Along the following discussion it will be useful to refer to two different unit cells, cell Z4 and cell Z1, which are defined in Figure 10a. Note that cell Z1, which is compatible with the ideal square-planar crystallographic structure, is not compatible with the AFM ground-state magnetic structure. However, it is a convenient reference cell to index the structural instabilities. Of course cell Z4 is compatible with both the crystallographic structure and the AFM order. As expected from the results of Figure 9, the electronic structures of the idealized and distorted structures are almost identical. The calculation of phonon modes for the Z4 cell, assuming the ideal high-symmetry planar configuration, results in two unstable modes with imaginary frequencies i96.7 cm^{-1} and i56.4 cm^{-1}, which in the following will be refereed to as the u and w modes, respectively. There are two additional modes which are quite low-energy-lying although they are not

(28) For the symmetry analysis we made use of the Bilbao Crystallographic Server program described in Kroumova, E.; Aroyo, M. I.; Perez Mato, J. M.; Kirov, A.; Capillas, C.; Ivantchev, S.; Wondratschek, H. *Phase Transitions* **2003**, *76*, 155.

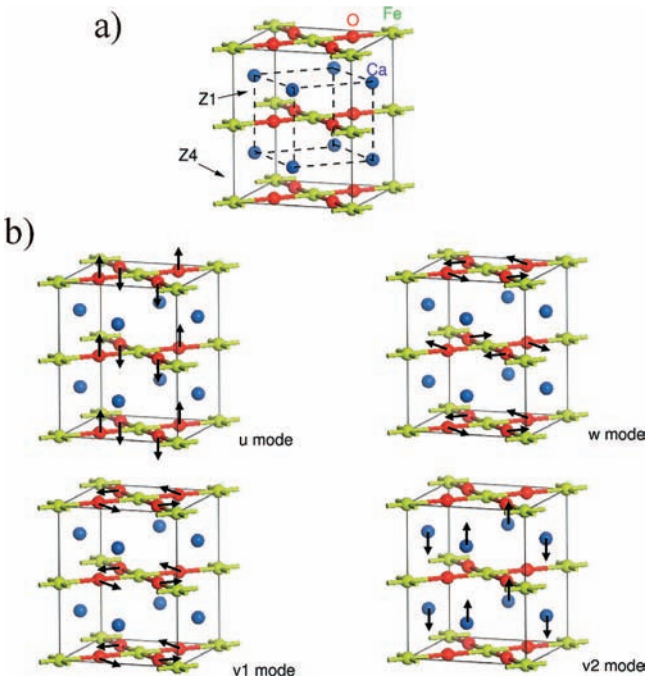

Figure 10. (a) Relationship between the unit cells (Z1 and Z4 contain one and four formula units respectively) useful for the analysis of the distortion in $CaFeO_2$. (b) Phonon modes relevant for understanding the origin of the distortion.

associated with an imaginary frequency which will be relevant for the analysis. These modes are at 112.8 cm^{-1} and 129 cm^{-1}, and in the following will be refereed to as the v1 and v2 modes. The nature of the four modes is schematically shown in Figure 10b The u mode is associated with an out-of-plane motion of the oxygen atoms so as to leave the iron atoms in a pseudotetrahedral coordination and is compatible with $q = (0, 0, 0)$ of cell Z1. Mode w is associated with an in-plane rotation of the FeO_4 squares which as shown in Figure 10b is compatible with $q = (1/2, 1/2, 1/2)$ of cell Z1. The v1 and v2 modes are respectively associated with in-plane rotations of the FeO_4 squares and out-of-plane motions of the calcium atoms. Both modes are compatible with $q = (1/2, 1/2, 0)$ of cell Z1.

With this information in mind we carried out a study of the different phases which may be obtained by freezing-in different combinations of these modes. The main conclusions of this study are the following: (a) the u instability clearly dominates over w, (b) once instability u condensates the v1 and v2 instabilities with $q = (1/2, 1/2, 0)$ become unstable and condense too, (c) the lowest-energy phase obtained is the experimentally observed structure. Let us note that, depending on the signs on the different combinations of the u, v1, and v2 modes, slightly different phases, though of slightly higher energies, may be obtained. Thus, it cannot be discarded that slightly different structures could be obtained if similar phases could be prepared with fourth- or fifth-row transition metals. In addition, it seems clear that the driving force for the distortion is the attempt of the oxygen atoms to optimize their interaction with the calcium cations by leaving the Fe^{2+} in an incipient tetrahedral coordination, and only then do the concerted rotations of the FeO_4 units and out-of plane motion of the calcium atoms occur to reach the optimal coordination for both iron and calcium. One could think of an alternative distortion involving Fe−O−Fe bond angle bending without modifying the O−Fe−O bond angle of 180 °. Inspection of our results led to the identification of low-lying phonon modes of this type with frequencies around 130 cm^{-1}. Nevertheless, these modes do not provide an energetically favorable option because they lead to a lower-symmetry and less favorable environment for the Ca atoms.

Our analysis clearly suggests that the smaller size of the calcium as compared to strontium must be the key parameter in controlling the occurrence of the distortion. In order to check this point we performed the same type of calculations for $BaFeO_2$, starting from the planar configuration. We computed the phonons and obtained no unstable modes thus confirming that the FeO_2 layers must stay planar in this material. This clearly confirms that the small size of the Ca ion is essential in making the new type of layered structure exhibited by $CaFeO_2$ possible.

Concluding Remarks

Use of the calcium hydride based low-temperature reduction route has led to the discovery of a new type of layered structure containing infinite FeO_2 layers, $CaFeO_2$. This structure is related to the recently reported $SrFeO_2$ exhibiting infinite FeO_2 layers isostructural with those of the copper-based high-T_c superconductors. The study of the Mössbauer and XAS spectra of the whole solid solution $(Sr_{1-x}Ca_x)FeO_2$ shows that the $SrFeO_2$-type structure is retained for $0 \leq x \leq 0.8$; however for $x = 1$ a change in the structural and electronic properties corresponding to the new structure is detected. The coordination of the high-spin Fe^{2+} ions is considerably distorted from square-planar toward tetrahedra, a very uncommon situation for high-spin d^6 systems which to the best of our knowledge has only been found in one occasion. As for $SrFeO_2$, $CaFeO_2$ exhibits the *G*-type AFM ordering well above room temperature. However, there is only a 50 K reduction in T_N in spite of a relatively large deviation of the oxygen bridging angle from 180°. Thus, the AFM ordering is quite robust, something which is in contrast for instance with the situation for compounds of the $AMnO_3$ family (A = La and rare earth elements), where the magnetic ordering is strongly influenced by the in-plane ∠Mn−O−Mn angle.

The present results nicely illustrate how strongly the correlation between spin-state and stereochemistry in four-coordinate d^6 transition metal compounds may differ in molecular and extended systems. There is both theoretical and experimental evidence that the high-spin systems adopt the tetrahedral coordination in molecular systems[8] and this is something which may be understood even from a purely one-electron approach. In contrast, the $AFeO_2$ (A = Ca, Sr, Ba) layered oxides clearly prefer the square-planar coordination and only if the size of the cation is small enough to make it advantageous for the oxygen atoms to move out of the plane to optimize the bonding with the cations, a drift toward an incipient tetrahedral coordination is created. It would be interesting to examine if by use of larger fourth- or fifth- row transition metal atoms the distortion toward the tetrahedral coordination starts appearing for larger cations, and thus the more usual tetrahedral coordination for the high-spin systems can be recovered. However, let us point out that, even in that case, the origin of the structural preference in the molecular and extended systems would be different.

Acknowledgment. We thank Kenji Nemoto for the support of the neutron diffraction experiment, Kenichi Kato and Kim Jungeun for the support of the synchrotron X-ray diffraction experiment, and Tsuyoshi Kimura for helpful information. This work was supported by DGES-Spain (Projects FIS2006-12117-C04-01 and CSD2007-00041), Generalitat de Catalunya (Project 2005 SGR

683), and by Grants-in-Aid for Scientific Research on Priority Areas "Novel States of Matter Induced by Frustration" (No. 19052004) and "Invention of Anomalous Quantum Materials" (No. 16076210) from the Ministry of Education, Culture, Sports, Science and Technology of Japan. Y.T. was supported by the Japan Society for the Promotion of Science for Young Scientist, and the research fellowship of Global COE program, International Center for Integrated Research and Advanced Education in Materials Science, Kyoto University, Japan. We made use of the computational facilities provided by CESCA and CESGA. The XAS and synchrotron XRD measurements were performed at the facilities of BL39XU (Proposal No. 2008A-1972) and BL02B2 (Proposal No. 2008A-1713), respectively, in SPring-8 with the approval of the Japan Synchrotron Radiation Research Institute (JASRI).

JA8072269